Magnetic nanocomposites based on poly(styrene-b-butadiene-b-methyl methacrylate) and modified Fe_2O_3 nanoparticles

I. Barandiaran, G. Kortaberria*

"Materials + Technologies" Group, Universidad del Pais Vasco/Euskal Herriko Unibertsitatea, Plaza Europa 1, 20018 Donostia, Spain

*corresponding autor: Galder Kortaberria, Plaza Europa 1, 20018 Donostia, Spain. Tel: 0034 943017176; email: galder.cortaberria@ehu.eus

ABSTRACT

In this work an ABC-type triblock copolymer has been used to prepare magnetic organic/inorganic nanocomposites by selectively placing maghemite nanoparticles modified on their surface with different polymer brushes. As ABC-type triblock copolymers can be nanostructured resulting in different morphologies with three different nano-sized block domains, they constitute interesting templates for selectively host nanofillers on them. In this work magnetic nanoparticles have been surface-modified with PS and PMMA brushes following the *grafting through* method, in order to selectively place at PS and PMMA block domains of the nanostructured block copolymer. Morphological characterization of ABC-type copolymers presents a higher complexity than that of AB diblock or ABA-type triblock copolymers, as a higher amount of parameters controlling the nanostructuring process must be taken into consideration, especially the interaction parameters between blocks that are of crucial importance, besides block composition and solvent employed for film preparation. Morphology of neat block copolymer and nanocomposites with PS- and PMMA-modified nanoparticles has been analyzed by atomic force microscopy. Nanocomposites maintained the lamellar nanostructure of SBM triblock copolymer, with nanoparticles selectively placed into the desired domains, as it has been demonstrated by both AFM and DSC measurements. Magnetic characterization by vibrating sample magnetometry demonstrates that magnetic properties of nanoparticles have been successfully transferred to nanocomposites.

1. INTRODUCTION

Lasts years research about nanocomposites based on block copolymers and inorganic nanoparticles have attracted large attention. Many researchers have focused their

attention on this kind of nanomaterials due to their potential application in photonic band gap materials, solar cells, sensors, or high-density magnetic storage devices [1-4]. Most of the works in this research area are based on AB or ABA-type block copolymers as matrix for nanocomposite film preparation. In this way, Gutierrez et al. [5] used PS-*b*-PEO (poly(styrene-*b*-ethylene oxide)) diblock copolymer for successfully preparing conductive nanocomposites by confining inorganic TiO_2 nanoparticles in PEO block domains, obtaining attractive materials that could be used in the field of dye-sensitized solar cells. Xu et al. [6] prepared magnetic nanocomposites based on lamellar forming PS-*b*-PMMA (poly(styrene-*b*-methyl methacrylate)) matrix and PMMA-modified Fe_3O_4 nanoparticles while Metwalli et al. [7] investigated how PS-*b*-PEO copolymer worked as a pattern for directing agent in which cobalt nanowires were formed by sputter decomposition. Regarding ABA-type block copolymers, Etxeberria et al. [8] fabricated nanocomposites based on SBS (poly(styrene-*b*-butadiene-*b*-styrene)) copolymer and surface-modified CdSe nanoparticles, analyzing their conductive properties by electrostatic force microscopy. Czaniková et al. [9] used also this kind of triblock copolymer to study the photo-actuator behavior of nanocomposites based on SIS and multiwalled carbon nanotubes. Also in our previous works we used AB-type copolymers like PS-*b*-PCL (poly(styrene-*b*-ε-caprolactone)), PS-*b*-PMMA or PS-*b*-P4VP (poly(styrene-*b*-4-vinyl pyridine)) to host magnetic nanoparticles modified with PMMA or PS brushes [10-12].

Regarding ABC-type block copolymers, many works have been published on their morphological behavior both in bulk or thin films. Löbling et al. [13] analyzed the self-assembly of SBT (poly(styrene-*b*-butadiene-*b*-*tert*-butyl methacrylate)) copolymer in bulk, obtaining unusually broad stability regions. They focused on χ parameter, concluding that a proper combination of this parameter can control the phase behavior,

implying a minor influence of block volume fraction. Hückstädt et al. [14] investigated the influence of block sequence on the morphological behavior of SBV (poly(styrene-*b*-butadiene-*b*-2-vinyl pyridine)) and BSV (poly(butadiene-*b*-styrene-*b*-2-vinyl pyridine)) copolymers, concluding that block sequence is decisive. Morphologies generated for ABC-type copolymer thin films have also been investigated. Fukunaga et al. [15] analyzed the effect of substrates on the generated morphology, using two types of substrates, polyimide and oxide silicon, finding significant differences. Elbs et al. [16] studied the differences in the resulting structure depending on the solvent used for vapor annealing SVT (poly(styrene-*b*-2-vinyl pyridine-*b*-*tert*-butyl methacrylate)) triblock copolymer. Although ABC-type triblock copolymers morphology have been broadly investigated and they present higher versatility than AB or ABA-type ones due to the higher amount of nanostructures that can be formed, this type of copolymers have barely been used for nanocomposite generation. Choi et al. [17] analyzed the effect of ABA or ABC-type triblock copolymers and hydroxylation degree on organoclay dispersion, concluding that a proper functionalization improves considerably their dispersion. Toombes et al. [18] prepared PEP-*b*-PEO-*b*-PHMA (poly(ethylene-*alt*-propylene-*b*-ethylene oxide-*b*-*n*-hexyl methacrylate)) triblock copolymer/aluminosilicate hybrid materials with aluminosilicates confined at PEO domains, obtaining hexagonally patterned lamellar morphology in which lamellae were aligned parallel to the surface. Stefik et al. [19] used ABC-type copolymers for synthesizing highly ordered nanocomposites with alumino silicate and niobia sols, underlaying that copolymer removal enabled simple and direct synthesis of mesoporous oxide materials.

In this work organic/inorganic nanocomposites have been prepared based on poly(styrene-*b*-butadiene-*b*-methyl methacrylate) SBM copolymer and maghemite nanoparticles. These nanoparticles have been modified by *grafting through* method with

PS and PMMA brushes. This functionalization improves their dispersion through the copolymer and their selective placement into different domains. Morphologies of neat triblock copolymer and nanocomposites with PS- or PMMA-modified nanoparticles have been studied with atomic force microscopy (AFM). Thermal transitions of the copolymer were analyzed by differential scanning calorimetry (DSC), studying the differences between neat copolymer and nanocomposites. Magnetic characterization of the nanocomposites was also carried out by vibrating sample magnetometer (VSM), finding that nanoparticles transferred their magnetic properties to the nanocomposite after modification and dispersion into block copolymer. To the best of our knowledge, this is the first report on organic/inorganic hybrid nanocomposite films based on triblock copolymers and magnetic nanoparticles.

2. EXPERIMENTAL PART

2.1. Materials

Maghemite nanoparticles with a nominal size of 9 nm were purchased from Integram Technologies, Inc. 3-methacryloxypropyl trimethoxysilane (MPTS) with 98 % of purity was purchased from ABCR. The 2,2'-azobisisobutyronitrile (AIBN) initiator, used without further purification, was purchased from Aldrich. Styrene (S) and methyl methacrylate (MMA) monomers, both with a purity of 99 %, were also purchased from Aldrich and were distilled under reduced pressure over CaH_2 before use. SBM triblock copolymer, with a number average molecular weight M_n of 96.142 g/mol was kindly supplied by Repsol, with the following volumetric composition: f_{PS}=0.3, f_{PB}=0.4 and f_{PMMA}=0.3.

2.2. Nanoparticle modification

2.2.1. Silanization process

Maghemite nanoparticles were first modified with MPTS. This reaction implies a nucleophilic attack of –OH groups at nanoparticle surface to the Si atoms of MPTS. 0.05 g of nanoparticles and 10 μmol of silane were mixed by sonication into 40 mL of toluene. The reaction was carried out at inert atmosphere for 3 h at 60 ºC. Nanoparticles were subsequently washed with THF (elimination of monomer was checked by FTIR) and dried in vacuum for 72 h at 40 ºC.

2.2.2. *Grafting through* process

Once nanoparticles were silanized, their surface modification by *grafting through* method was carried out. Nanoparticles were modified with PS and PMMA brushes, in order to analyze the effect of functionalization on the morphology of nanostructured SBM and the selective positioning of nanoparticles into desired domains. 0.02 g of silanized Fe_2O_3 nanoparticles and 0.1 g of AIBN were dispersed into 40 mL of toluene and then 2 mL of S or MMA monomer were added. Reaction was carried out at inert N_2 atmosphere at 70 ºC for 5 h. Modified nanoparticles were subsequently washed with THF (elimination of monomer was checked by FTIR) and dried in vacuum for 72 h at 40 ºC.

2.3. Nanocomposite preparation

Nanocomposites were prepared by mixing SBM copolymer with PS- and PMMA-modified nanoparticles. Nanoparticles were first dispersed in toluene for 2 h by sonication, and then SBM block copolymer was added. Thin films of neat block copolymer and nanocomposites were then prepared by casting SBM solutions in toluene with a concentration of 5 wt% onto Si(100) wafers. Nanocomposites with 1, 2, and 5 wt% of nanoparticles were prepared.

2.4. Characterization techniques

Fourier transformed infrared spectroscopy (FTIR) was carried out with a Nicolet Nexus 600 FTIR spectrometer, performing 20 scans with a resolution of 4 cm^{-1}.

Thermogravimetric analysis (TGA) was performed with a Mettler Toledo TGA/SDTA851 instrument, running from room temperature to 750 ºC with a heating rate of 10 ºC/min.

Surface morphologies obtained for different films were studied by AFM with a scanning probe microscopy AFM Dimension ICON of Bruker, operating in tapping mode (TM–AFM). An integrated silicon tip/cantilever, from the same manufacturer, having a resonance frequency of around 300 kHz, was used. Measurements were performed at a scan rate of 1 Hz/s, with 512 scan lines.

Thermal transition temperatures of neat SBM triblock copolymer and SBM/Fe_2O_3 nanocomposites with PS- or PMMA-modified nanoparticles were determined by using a DSC (Mettler Toledo DSC 822e), with nitrogen flow of 10 mL/min. Dynamic scans were performed from 25 to 160 °C with a heating rate of 10 °C/min after carrying out a previous heating scan to delete the thermal history of the samples.

Magnetic measurements were performed at VSM. The VSM (CFMS, Cryogenic Ltd) has a superconducting magnet of 14 T, and was used to carry out ZFC/FC measurements and also for measuring hysteresis loops at 2, 225 and 300 K.

3. RESULTS AND DISCUSSION

3.1. Characterization of modified nanoparticles

Before functionalization of nanoparticles with polymeric brushes, nanoparticle surface was silanized. The right attachment of silane to nanoparticle surface is of vital importance, as the addition of MPTS results in vinyl group-terminated maghemite nanoparticles for

the subsequent polymerization of PS and PMMA brushes [20, 21]. The success of silanization process was probed by FTIR and TGA measurements. In Figure 1 FTIR spectra of silanized, PS-modified and PMMA-modified nanoparticles can be seen. For silanized nanoparticles the appearance of bands related with the main bonds of MPTS can be seen in the spectrum: C=O stretching vibration at 1704 cm^{-1}, C-O-C stretching deformation vibration at 1329 and 1300 cm^{-1}, and Si-O-Fe stretching vibration at 1176 and 1011 cm^{-1}, indicating the presence of MPTS attached to the surface [22]. After silanization, nanoparticles were modified with polymeric brushes by *grafting through* method. The presence of PS brushes into the surface was also probed, with the appearance of PS main bands in the FTIR spectrum of PS-modified nanoparticles: C-H aromatic stretching vibration (3023 cm^{-1}, inner part of the figure), C-C stretching frequency of the ring in plane (1600 cm^{-1}), C-C stretching vibration of the ring in plane (1494 cm^{-1}) and C-H out of plane bending vibration of the ring (700 cm^{-1}), can be seen [23, 24]. Moreover, the modification of nanoparticle surface with PMMA brushes was also probed by the presence of an intense band corresponding to the stretching vibration of carbonyl group in the methacrylate at 1723 cm^{-1}, together with the appearance of bands related to the stretching vibration of C-O-C at 1263, 1243, 1191 and 1151 cm^{-1} [25].

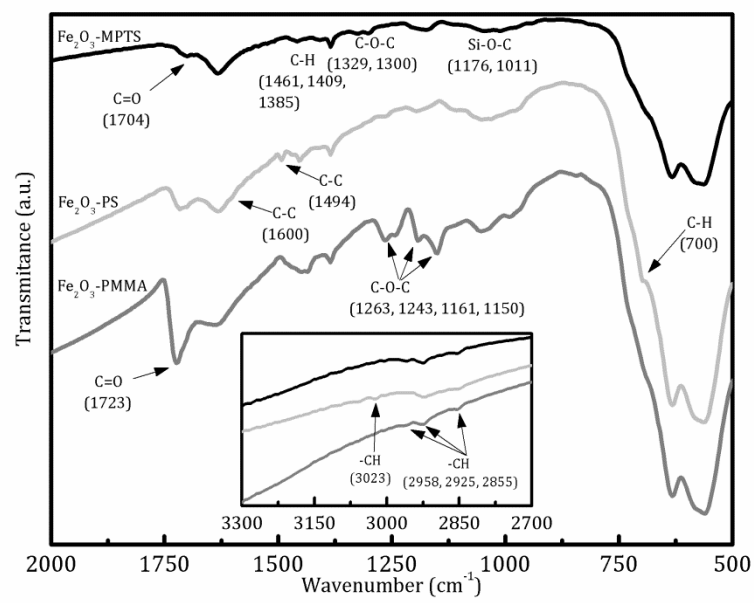

TGA thermograms (Figure 2) also confirm the modification of pristine, silanized and brush-modified nanoparticles. Weight loss of unmodified nanoparticles is related to physisorbed water (until 120 ºC) and surface -OH degradation (above 120 ºC) [26]. For the thermogram corresponding to silane-modified nanoparticles, an increase of weight loss is appreciated, indicating the thermal degradation of MPTS. A surface density of 2.8 molecules/nm^2 has been calculated for the silane following the method used by Bartholome et al. [27]. A direct comparison of the surface density of hydroxyl groups (8.1 molecules/nm^2) and that of the silane on the surface yielded a reaction efficiency of 34.5 %. Moreover, weight losses related to the degradation of PS and PMMA brushes can be clearly seen, thus probing the presence of polymer at nanoparticle surface.

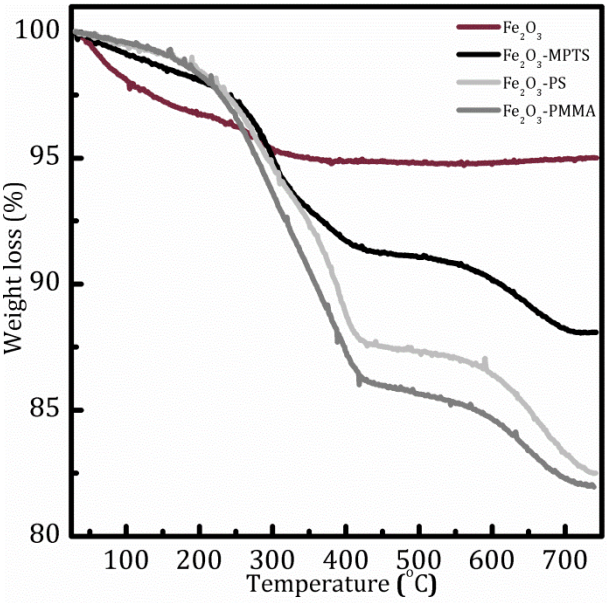

3.2. Characterization of nanocomposites

The first step was to characterize surface morphologies obtained for neat triblock copolymer films. Figure 3 shows AFM images for neat copolymer film, where lamellar morphology can be seen. Lamellar is one of the morphologies that can be obtained for ABC-type triblock copolymer films [28]. Stadler et al. [29] investigated the morphologies formed for SBM and their hydrogenated analogues (SEBM), highlighting the importance of interaction parameters in order to determine the morphologies of ABC copolymers, when comparing with AB diblock or ABA triblock ones, for which the main factor determining the morphology is the composition. However, they indicated that interaction parameters made the difference mainly when the amount of the middle block was low, around 6 wt%. For copolymers with block ratios similar to those analyzed in this work (30/40/30 in volume) they pointed out that a lamellar morphology could be expected. In AFM images of Figure 3, PB domains can be clearly identified as darker ones because it presents the lowest modulus [30, 31], while PS and PMMA domains cannot be clearly differentiated.

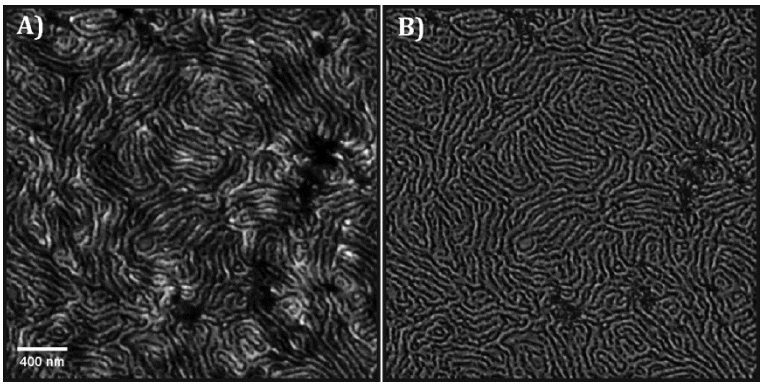

In order to better visualize the morphology and differentiate between PS and PMMA domains, amplified height and phase AFM images of neat triblock copolymer thin film are shown in Figure 4. As it can be seen, PS and PMMA domains can be better distinguished as PMMA domains appear brighter than PS ones due to its higher modulus [31]. The profiles obtained for height and phase images, also shown in Figure 4, help in distinguishing between SBM domains. In those profile images, four domains stand up from PB ones, placed at the bottom as they are the softener; they correspond to PS and PMMA domains, which can be separated into two pairs depending on their height, placed alternatively. The highest one represents PMMA domains, as it presents the highest modulus. So it can be concluded that SBM triblock copolymer assembles into a lamellar morphology with S-B-M-B sequence and an average interlamellar distance of ~71 nm, although some interruptions of the sequence can be appreciated (marked with a circle in Figure 4), as PS and PMMA domains appear joined. Scheme 1 shows a schematic representation of this lamellar structure.

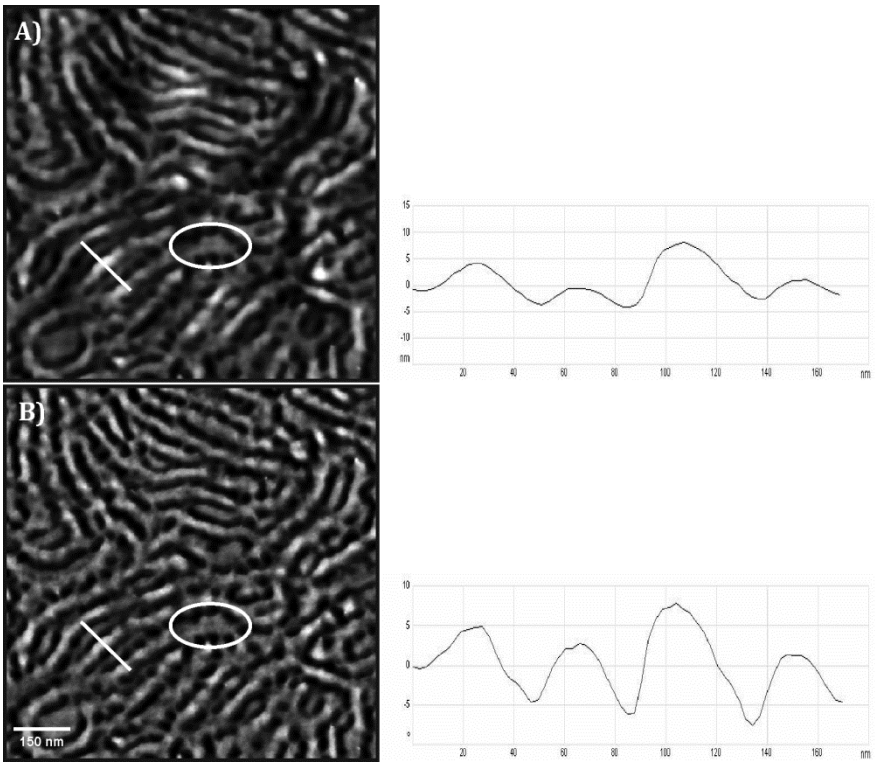

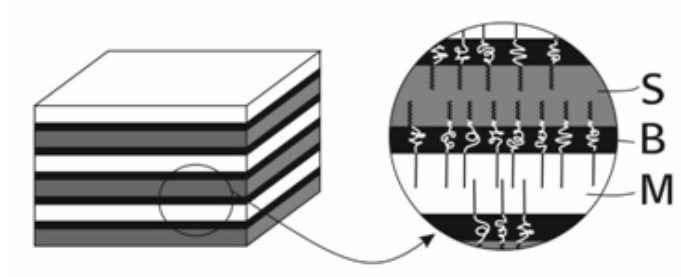

Nanocomposites were prepared by adding magnetic nanoparticles modified with PS or PMMA brushes to SBM matrix. In Figures 5 and 6 AFM images for nanocomposites with 1, 2 and 5 wt% of PS- and PMMA-modified nanoparticles, respectively, can be seen. Lamellar morphology of neat triblock copolymer is maintained with nanoparticle addition, independently of the modification. Moreover, nanoparticles are well dispersed through the triblock copolymer matrix, without the presence of remarkable aggregates. For a better visualization of the effect of nanoparticles on film morphology, amplified height and phase images of nanocomposite thin films with 5 wt% of nanoparticles are shown in Figure 7, together with the corresponding height profile.

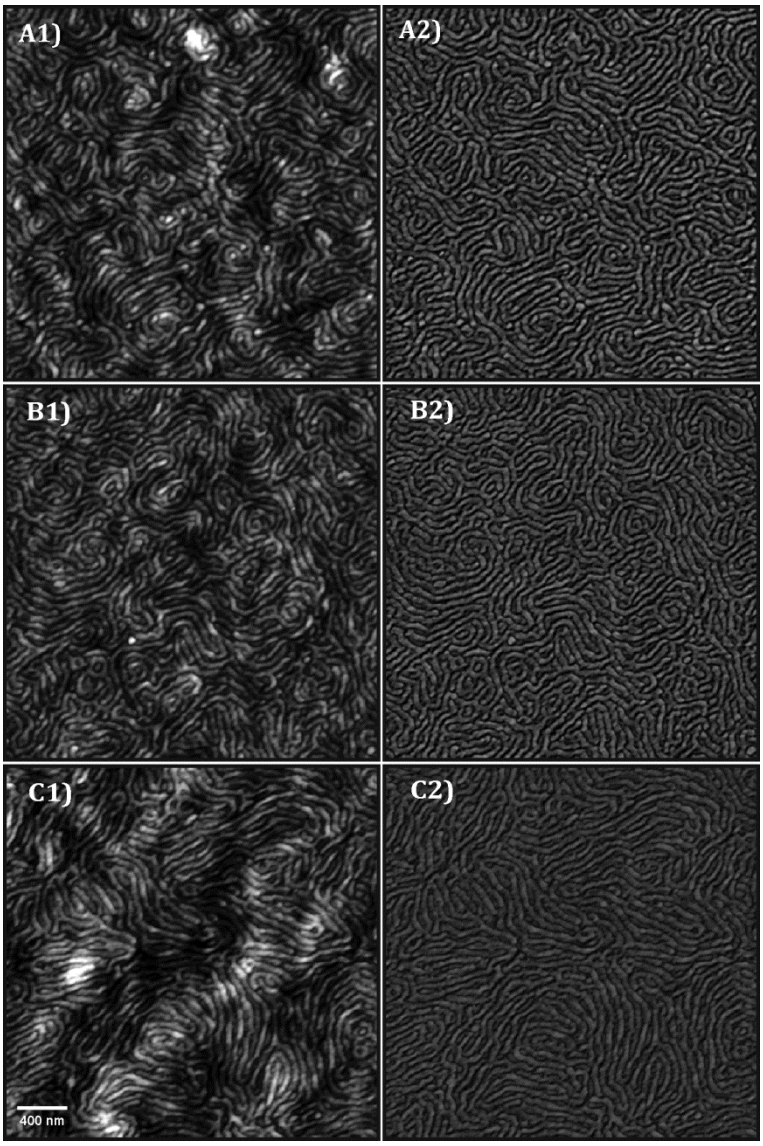
A1)
A2)
B1)
B2)
C1)
C2)
400 nm

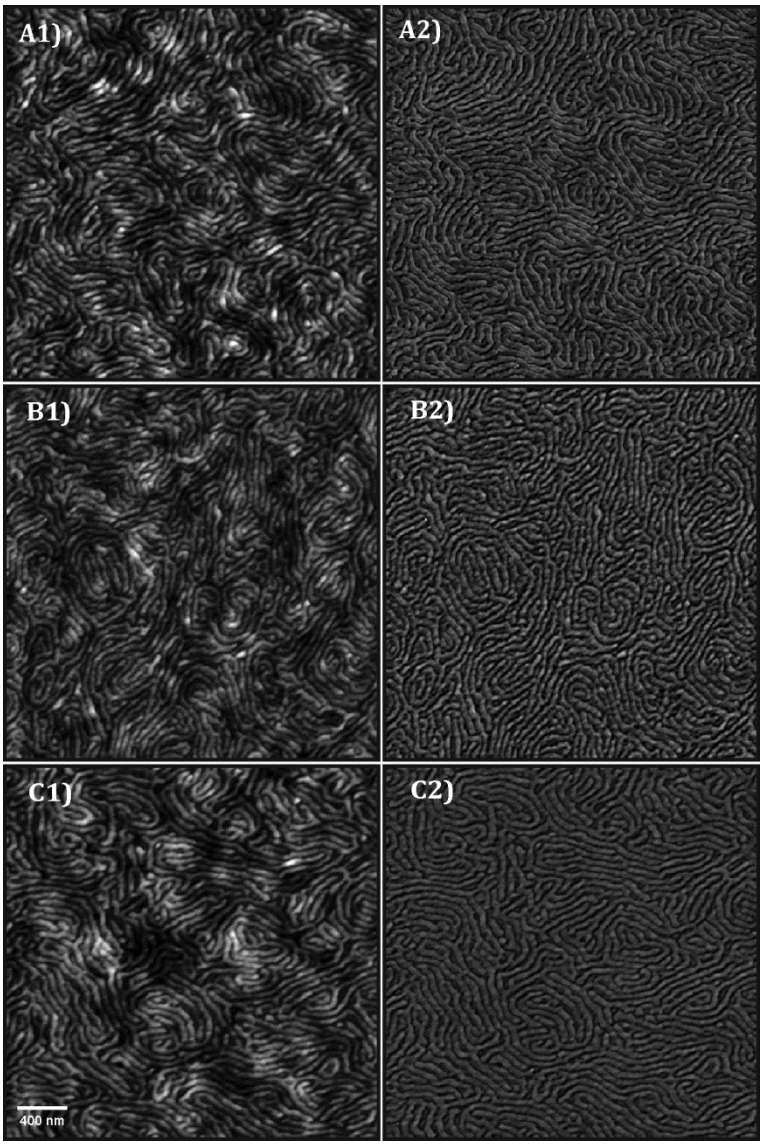

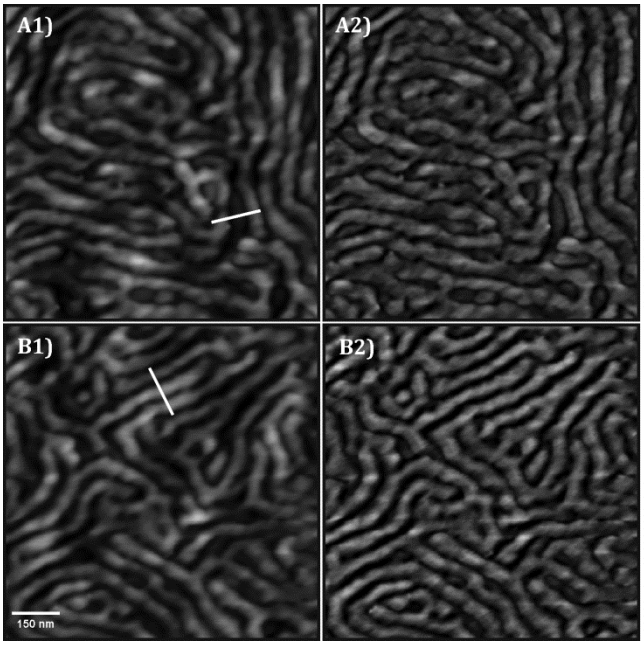

A3)

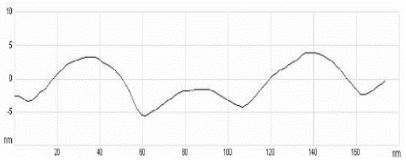

B3)

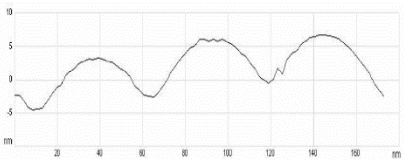

In both cases, although lamellar morphology is maintained after nanoparticle addition, it appears more disrupted. When PS-modified nanoparticles are added, PS domains can be better distinguished in AFM images, comparing to the images corresponding to nanocomposites with PMMA-modified nanoparticles. When PMMA-modified nanoparticles are added, it seems that PS and PMMA domains tend to join. If the profile images are compared with those of Figure 4, it can be clearly seen that PS and PMMA domains tend to swollen with nanoparticle addition. All profiles are around 170 nm length. In these profiles, for neat BCP four domains can be separated, identified as PMMA (higher ones) and PS (lower ones), but when nanoparticles are added, only 3 domains can be observed. This fact could indicate that nanoparticles are located at PS and PMMA domains, as their placement at those domains would increase the respective domain volume [32].

Differences found between neat BCP and nanocomposite thin film nanostructures could be due to the effect of nanoparticles on system thermodynamics, as they can affect the interaction forces between blocks. Lo et al. concluded that nanoparticle addition weakened the phase segregation between blocks [33], while Lin et al. induced the self-assembly of BCP by adding inorganic nanoparticles, due to a strengthening of interaction forces between blocks [34]. Those examples show the complexity of understanding nanostructures based on triblock copolymers and inorganic nanoparticles. As it was mentioned before, when PS- and PMMA-modified nanoparticles are added, more notoriously with PMMA-modified ones, PS and PMMA domains of the triblock tend to join. This could be due to the low repulsive forces between PS and PMMA blocks. According to interaction parameter values, $\chi_{PMMA/PS}$= 0.0044 is much lower than $\chi_{PS/PB}$= 0.045 and $\chi_{PMMA/PB}$= 0.071 [29], which could facilitate the mixture of PS and PMMA blocks. Hückstädt et al. [14] analyzed the effect of block sequence on obtained

nanostructure, analyzing first SBV and BSV copolymer nanostructures with three strongly incompatible components, finding that were affected by the block sequence. Then they compared obtained results with those for SBM and BSM copolymers, in which the incompatibility between PS and PMMA blocks was low. Due to this low incompatibility, PS and PMMA tended to mix. On the other hand, the incompatibility between PMMA and PB blocks, higher than that among PS and PB ones, could explain the reason for PS and PMMA domains to be better distinguished when PS-modified nanoparticles are added than when PMMA-modified ones are added. Larger incompatibilities between blocks lead to the generation of larger interfaces [13].

In order to reinforce the importance of nanoparticle surface functionalization when preparing organic/inorganic nanocomposites based on BCP, nanocomposites with pristine nanoparticles were also prepared. In Figure 8 AFM images of the nanocomposite with 5 wt% of pristine nanoparticles can be seen with big nanoparticle aggregates. Different areas of the thin film were analyzed, and the presence of aggregates was repetitive. With pristine nanoparticle addition the lamellar nanostructure of the triblock copolymer is maintained, but their dispersion is not as good as for modified nanoparticles.

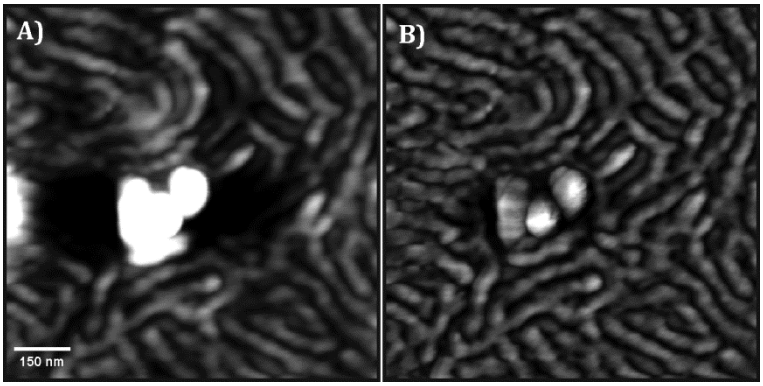

DSC thermograms of neat SBM and nanocomposites with PMMA- and PS-modified nanoparticles (1, 2 and 5 wt%) are shown in Figure 9. In the analyzed temperature range,

two glass transition temperatures (T_g) can be distinguished. For the neat copolymer, they appear at 102 and 131 ºC, corresponding to PS and PMMA blocks, respectively. With nanoparticle addition, T_g values seem to be very similar, with a slight increase of the T_g of PS block in nanocomposites with PS-modified nanoparticles to 104 ºC, and that of the T_g of PMMA block in nanocomposites with PMMA-modified nanoparticles to 133 ºC. This fact could be related to the presence of PS-modified nanoparticles at PS domains and PMMA-modified ones at PMMA domains, as the presence of the nanoparticles would hinder chains mobility, resulting in a higher T_g for the block [35].

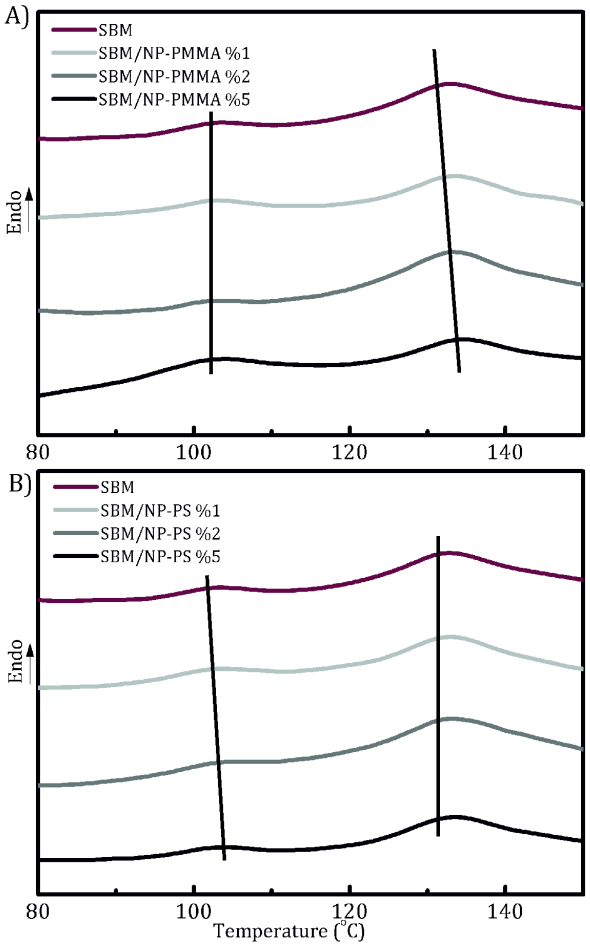

3.3. Magnetic characterization

Figure 10 shows the ZFC/FC curves of nanocomposites with 1 and 5 wt% of PS- and PMMA-modified nanoparticles obtained from VSM measurements. These

nanocomposites present superparamagnetic behavior at room temperature and ferromagnetic at lower temperature; magnetic properties of nanoparticles have been transferred to nanocomposites successfully, despite surface functionalization. The blocking temperature, T_B, in all nanocomposites is around 200 and 250 K, and it does not vary with nanoparticle concentration. According to Néel-Brown expression ($T_B = \frac{K_{eff}V}{30k_B}$) T_B depends on the size of the nanoparticles, so the fact that the value of T_B is maintained by increasing nanoparticle concentration could suggest that the size of the nanoparticles is maintained, or in this case, the size of aggregates. As it was pointed out in a previous work, when nanoparticles are functionalized by *grafting through* method instead of being located individually, they could be bonded together with several polymer chains, creating a kind of network [34]. So it seems that aggregates were formed during nanoparticle modification and not during nanocomposite preparation, as the size of possible aggregates present in nanocomposites is very similar, and are not detected by AFM as were those formed by unmodified nanoparticles.

M *vs* B curves were also measured for nanocomposites with 5 wt% of PS- and PMMA-modified nanoparticles, as it can be seen in Figure 11. In both cases nanocomposites have a hysteretic loop at 2 K, with a coercivity of approximately 315 Oe, and remanence between $1.6 \cdot 10^{-4}$ and $2.1 \cdot 10^{-4}$ emu. Near to T_B (225 K) both nanocomposites become un-hysteretic, and coercivity and remanence become zero. At room temperature, both coercivity and remanence also become zero, proving the superparamagnetic behavior of the nanocomposites. Again, it has been demonstrated that magnetic properties of the nanoparticles have been successfully transferred to nanocomposites, despite the modification of nanoparticle surface with polymeric brushes.

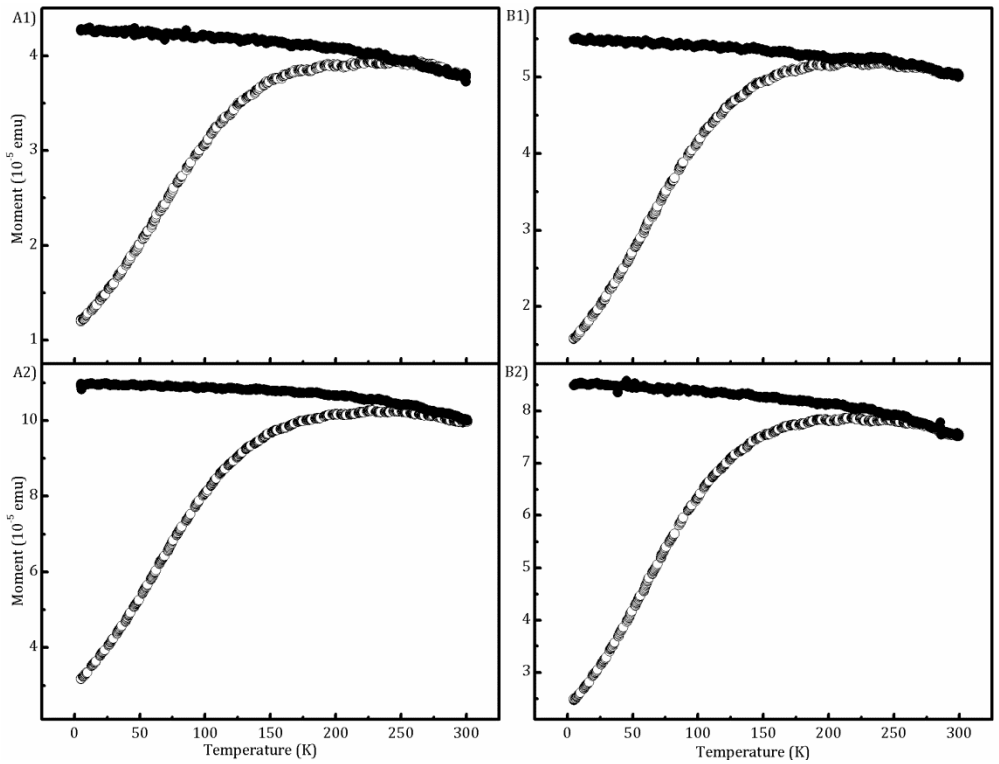

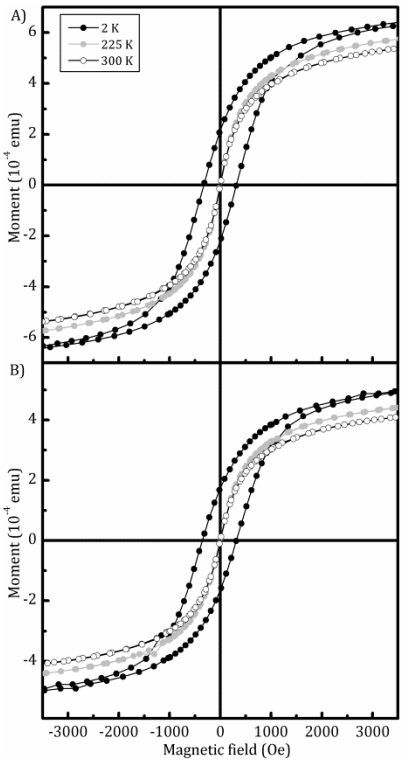

4. CONCLUSIONS

The main goal of this work is to demonstrate the potential of ABC-type block copolymers to prepare inorganic/organic nanomaterials with interesting properties. This kind of

copolymers can be exceptional candidates for synthesizing organic/inorganic hybrid nanocomposites, as they provide the possibility to host nanoparticles with different functionalities, opening broader possibilities for the synthesis of hybrid materials. In this work nanocomposites based on SBM copolymer with magnetic nanoparticles selectively placed on PS or PMMA domains depending on their functionalization with the corresponding brushes. Results obtained in this work have shown that *grafting through* method is useful for functionalizing nanoparticles with both polymer brushes, making possible their placement at the desired domains, as it has been demonstrated by AFM and DSC measurements. Complexity of ABC-type copolymers has also been explored. As their self-assembly is affected by more parameters than that of diblock or ABA-type triblock copolymer, the interpretation of nanostructures is more complicated. Their versatility related with the high amount of nanostructures that can generate, and their ability to host different nanoparticles, makes them very interesting materials for nanocomposite fabrication, and, as only a few works can be found about, it constitutes an interesting topic for further research. Finally, the superparamagnetic behavior of nanocomposites has been also demonstrated by magnetic measurements, proving that magnetic properties of nanoparticles have been transferred to nanocomposites.

5. AKNOWLEDGEMENTS

Financial support from the Basque Country Government (Grupos Consolidados, IT-776-13) and the Ministry of Economy and Competitiveness (MAT 2012-31675) is gratefully acknowledged. The technical and human support provided by SGIker of UPV/EHU is also acknowledged. I.B. thanks Euskal Herriko Unibertsitatea/Universidad del País Vasco for Ph.D Fellowship (Becas de Formación de Investigadores 2011 (PIF/UPV/11/030)).

6. REFERENCES

[1] M.R. Bockstaller, R.A. Mickiewicz, E.L. Thomas, Block copolymer nanocomposites: perspectives for tailored functional materials, Adv. Mater. 17 (2005) 1331-1349.

[2] S.B. Darling, N.A. Yufa, A.L. Cisse, S.D. Bader ,S.J. Sibener, Self-organization of FePt nanoparticles on photochemically modified diblock copolymer templates, Adv. Mater. 17 (2005) 2446-2450.

[3] S. Park, D.H. Lee, J. Xu, B. Kim, S.W. Hong, U. Jeong, T. Xu, T.P. Russell, Macroscopic 10-Terabit–per– Square-Inch Arrays from Block Copolymers with Lateral Order, Science 323 (2009) 1030-1033.

[4] Y.H. Jang, X. Xin, M. Byun, Y.J. Jang, Z. Lin, D.H. Kim, An Unconventional Route to High-Efficiency Dye-Sensitized Solar Cells via Embedding Graphitic Thin Films into TiO_2 Nanoparticle Photoanode, Nano Lett. 12 (2012) 479-485.

[5] J. Gutierrez, A. Tercjak, I. Mondragon, Conductive Behavior of High TiO_2 Nanoparticle Content of Inorganic/Organic Nanostructured Composites, J. Am. Chem. Soc. 132 (2010) 873-878.

[6] C. Xu, K. Ohno, V. Ladmiral, D.E. Milkie, J.M. Kikkawa, R.J. Composto, Simultaneous Block Copolymer and Magnetic Nanoparticle Assembly in Nanocomposite Films, Macromolecules 42 (2009) 1219-1228.

[7] E. Metwalli, V. Körstgens, K. Schlage, R. Meier, G. Kaune, A. Buffet, S. Couet, S.V. Roth, R. Röhlsberger, P. Müller-Buschbaum, Cobalt Nanoparticles Growth on a Block Copolymer Thin Film: A Time-Resolved GISAXS Study, Langmuir 29 (2013) 6331-6340.

[8] H. Etxeberria, A. Tercjak, I. Mondragon, A. Eceiza, G. Kortaberria, Electrostatic force microscopy measurements of CdSe-PS nanoparticles and CdSe-PS/poly(styrene-b-butadiene-b-styrene) nanocomposites, Colloid Polym Sci 292 (2014) 229-234.

[9] K. Czaniková, M. Ilcíková, I. Krupa, M. Micusík, P. Kasák, E. Pavlova, J. Mosnácek, Jr D. Chorvát, M. Omastová, Elastomeric photo-actuators and their investigation by confocal laser scanning microscopy, Smart Mater. Struct. 22 (2013) 104001 (10pp).

[10] I. Barandiaran, A. Cappelletti, M. Strumia, A. Eceiza, G. Kortaberria, Generation of nanocomposites based on (PMMA-b-PCL)-grafted Fe2O3 nanoparticles and PS-b-PCL block copolymer, European Polymer Journal 58 (2014) 226–232.

[11] I. Barandiaran, G. Kortaberria, Selective placement of magnetic Fe_3O_4 nanoparticles into the lamellar nanostructure of PS-b-PMMA diblock copolymer, European Polymer Journal 68 (2015) 57-67.

[12] I. Barandiaran, G. Kortaberria, Synthesis and characterization of nanostructured PS-b-P4VP/Fe_2O_3 thin films with magnetic properties prepared by solvent vapor annealing, RSC Adv. 5 (2015) 95840-95846.

[13] T.I. Löbling, P. Hiekkataipale, A. Hanisch, F. Bennet, H. Schmalz, O. Ikkala, A.H. Gröschel, A.H.E. Müller, Bulk morphologies of polystyrene-block-polybutadiene-block-(tert-butyl methacrylate) triblock terpolymers, Polymer 72 (2015) 479-489.

[14] H. Hückstädt, A. Göpfert, V. Abetz, Influence of the block sequence on the morphological behavior of ABC triblock copolymers, Polymer 41 (2000) 9089-9094.

[15] K. Fukunaga, T. Hashimoto, H. Elbs, G. Krausch, Self-Assembly of a Lamellar ABC Triblock Terpolymer Thin Film. Effect of Substrates, Macromolecules 36 (2003) 2852-2861.

[16] H. Elbs, C. Drummer, V. Abetz, G. Krausch, Thin Film Morphologies of ABC Triblock Copolymers Prepared from Solution, Macromolecules 35 (2002) 5570-5577.

[17] S. Choi, K.M. Lee, C.D. Han, Effects of Triblock Copolymer Architecture and the Degree of Functionalization on the Organoclay Dispersion and Rheology of Nanocomposites, Macromolecules 37 (2004) 7649-7662.

[18] G.E.S. Toombes, S. Mahajan, M. Thomas, P. Du, M.W. Tate, S.M. Gruner, U. Wiesner, Hexagonally Patterned Lamellar Morphology in ABC Triblock Copolymer/Aluminosilicate Nanocomposites, Chem. Mater. 20 (2008) 3278-3287.

[19] M. Stefik, S. Mahajan, H. Sai, T.H. Epps, F.S. Bates, S.M. Gruner, F.J. DiSalvo, U. Wiesner, Ordered Three- and Five-ply Nanocomposites from ABC Block Terpolymer Microphase Separation with Niobia and Aluminosilicate Sols. Chem. Mater 21 (2009) 5466-5473.

[20] M. Kim, C.K. Hong, S. Choe, S.E. Shim, Synthesis of polystyrene brush on multiwalled carbon nanotube treated with $KMnO_4$ in the presence of phase-transfer catalyst, J Polym Sci Part A: Polym Chem 45 (2007) 4413-4420.

[21] S. Rahimi-Razin, V. Haddadi-Asl, M. Salami-Kalajahi, F. Behboodi-Sadabad, H. Roghani-Mamaqani, Matrix-grafted multiwalled carbon nanotubes/poly(methyl methacrylate) nanocomposites synthesized by in situ RAFT polymerization: A kinetic study. Int. J. Chem. Kinet. 44 (2012) 555-569.

[22] M.A. Rodriguez, M.J. Liso, F. Rubio, J. Rubio, J.L. Oteo, Study of the reaction of γ-methacryloxypropyltrimethoxysilane (γ-MPS) with slate surfaces, Journal of Material Science 35 (1999) 3867-3873.

[23] Y. Sun, X. Ding, Z. Zheng, X. Cheng, X. Hu, Y. Peng, Surface initiated ATRP in the synthesis of iron oxide/polystyrene core/shell nanoparticles, Eur Polym J 43 (2007) 762-772.

[24] H. Etxeberria, I. Zalakain, R. Fernandez, G. Kortaberria, I. Mondragon, Controlled placement of polystyrene-grafted CdSe nanoparticles in self-assembled block copolymers, Colloid Polym Sci 291 (2013) 633-640.

[25] H. Yan, X.-h. Zhang, L.-q. Wei, X.-g. Liu, B.-s. Xu, Hydrophobic magnesium hydroxide nanoparticles via oleica cid and poly(methyl methacrylate)-grafting surface modification, Powder Technology 193 (2009) 125-129.

[26] R. Mueller, H.K. Kammler, K. Wegner, S.E. Pratsinis, OH Surface Density of SiO_2 and TiO_2 by Thermogravimetric Analysis, Langmuir 19 (2003) 160-165.

[27] C. Bartholome, E. Beyou, E. Bourgeat-Lami, P. Chaumont, N. Zydowicz, Nitroxide-Mediated Polymerizations from Silica Nanoparticle Surfaces: "Graft from" Polymerization of Styrene Using a Triethoxysilyl-Terminated Alkoxyamine Initiator, Macromolecules 36 (2003) 7946-7952.

[28] U. Nagpal, F.A. Detcheverry, P.F. Nealey, J.J. de Pablo, Morphologies of Linear Triblock Copolymers from Monte Carlo Simulations, Macromolecules 44 (2011) 5490-5497.

[29] R. Stadler, C. Auschra, J. Beckmann, U. Krappe, I. Voigt-Martin, L. Leibler, Morphology and thermodynamics of symmetric poly(A-b-B-b-C) triblock copolymers, Macromolecules 28 (1995) 3080-3097.

[30] J. Bai, Z. Shi, J. Yina, M. Tian, A simple approach to preparation of polyhedral oligomeric silsesquioxane crosslinked poly(styrene-b-butadiene-b-styrene) elastomers with a unique micro-morphology via UV-induced thiol–ene reaction, Polym. Chem. 5 (2014) 6761-6769.

[31] C. Xu, K. Ohno, V. Ladmiral, D.E. Milkie, J.M. Kikkawa, R.J. Composto, Simultaneous block copolymer and magnetic nanoparticle assembly in nanocomposite films, Macromolecules 42 (2009) 1219-1228.

[32] J. Gutierrez, I. Garcia, A. Tercjak, I. Mondragon, The effect of thermal and vapor annealing treatments on the self-assembly of TiO_2/PS-b-PMMA nanocomposites generated via the sol-gel process, Nanotechnology 20 (2009) 225603 (9 pp).

[33] C.-T. Lo, Lee B., V.G. Pol, N.L. Dietz Rago, S. Seifert, R.E. Winans, P. Thiyagarajan, Effect of Molecular Properties of Block Copolymers and Nanoparticles on the Morphology of Self-Assembled Bulk Nanocomposites, Macromolecules 40 (2007) 8302-8310.

[34] Y. Lin, V.K. Daga, E.R. Anderson, S.P. Gido, J.J. Watkins, Nanoparticle-Driven Assembly of Block Copolymers: A Simple Route to Ordered Hybrid Materials, J. Am. Chem. Soc. 133 (2011) 6513-6516.

[35] L. Cano, J. Gutierrez, A. Tercjak, Rutile TiO_2 Nanoparticles Dispersed in a Self-Assembled Polystyrene-b-polymethyl Methacrylate Diblock Copolymer Template, J. Phys. Chem. C 117 (2013) 1151-1156.

CAPTIONS

Figure 1. Infrared spectrum of silanized, PS-modified and PMMA-modified nanoparticles

Figure 2. TGA thermograms of pristine, silanized, PS-modified and PMMA-modified nanoparticles

Figure 3. AFM height (A) and phase (B) images of SBM thin film

Figure 4. AFM height (A) and phase (B) images of SBM thin film with corresponding profile images

Figure 5. AFM height (1) and phase (2) images of nanocomposites with A) 1, B) 2 and C) 5 wt% of PS-modified nanoparticles

Figure 6. AFM height (1) and phase (2) images of nanocomposites with A) 1, B) 2 and C) 5 wt% of PMMA-modified nanoparticles

Figure 7. AFM height (1), phase (2) and profile (3) images of nanocomposites with 5 wt% of A) PS- and B) PMMA-modified nanoparticles

Figure 8. AFM height (A) and phase (B) images of nanocomposite thin film with 5 wt% of pristine nanoparticles

Figure 9. DSC thermograms of neat SBM and nanocomposites

Figure 10. ZFC/FC curves at 100 Oe of nanocomposites with (A) PS- and (B) PMMA-modified (1) 1 wt% and (2) 5 wt% of nanoparticles

Figure 11. M *vs* B curves at 2, 225 and 300 K for nanocomposites with 5 wt% of A) PS- and B) PMMA-modified nanoparticles

Scheme 1. Schematic representation of the formed lamellar nanostructure